ACS OMEGA

Article

http://pubs.acs.org/journal/acsodf

Effect of Vitamin E and a Long-Chain Alcohol *n*-Octanol on the Carbohydrate-Based Nonionic Amphiphile Sucrose Monolaurate—Formulation of Newly Developed Niosomes and Application in Cell Imaging

Arpita Roy,[†] Arghajit Pyne,[†] Pallabi Pal,[‡] Santanu Dhara,[‡] and Nilmoni Sarkar*[,†]

[†]Department of Chemistry and [‡]School of Medical Science and Technology, Indian Institute of Technology Kharagpur, Kharagpur 721302, West Bengal, India

Supporting Information

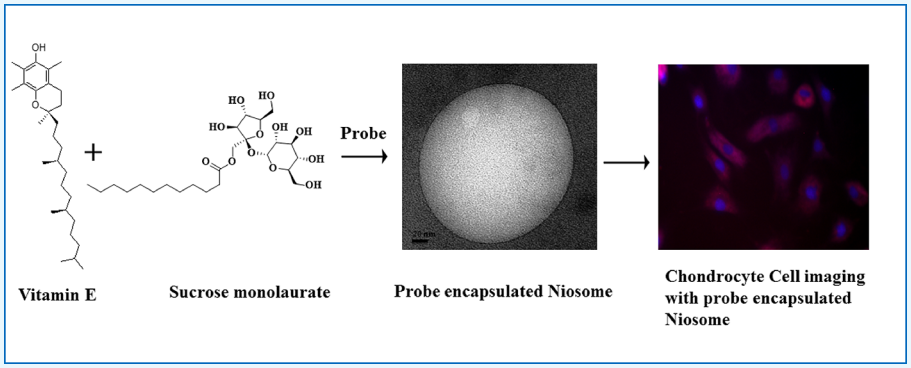

ABSTRACT: We have introduced new niosome formulations using sucrose monolaurate, vitamin E and *n*-octanol as independent additives. Detailed characterization techniques including turbidity, dynamic light scattering, transmission electron microscopy, ξ potential, and proton nuclear magnetic resonance measurements have been introduced to monitor the morphological transition of the carbohydrate-based micellar assembly into niosomal aggregates. Moreover, microheterogeneity of these niosomal aggregates has been investigated through different fluorescence spectroscopic techniques using a hydrophobic probe molecule coumarin 153 (C153). Further, it has been observed that vitamin E and octanol have an opposing effect on the rotational motion of C153 in the respective niosome assemblies. The time-resolved anisotropy studies suggest that incorporation of vitamin E and octanol into the surfactant aggregates results in slower and faster rotational motion of C153, respectively, compared to the micellar assemblies. Moreover, the ability to entrap a probe molecule by these niosomes is utilized to encapsulate and deliver the anticancer drug doxorubicin inside the mammalian cells which is monitored through fluorescence microscopic images. Interestingly, the niosome composed of vitamin E demonstrated better cytocompatibility toward primary chondrocyte cell lines compared to the octanol-forming niosome.

1. INTRODUCTION

The structural and morphological uniqueness of liposomes formed from phospholipids has created significant interests regarding the applications in pharmaceuticals and cosmetic industries, microreactors, soft templates for synthesizing various materials, and also as a model for the cell membrane.[1−10] Therefore, in the last few decades, these phospholipid-containing liposomes are extensively used as gene and drug delivery vehicles.[11−13] Although it is documented that phospholipid vesicles are nontoxic and can increase the therapeutic effects and drug stability, sometimes its applicability becomes limited because of the possibility of oxidative and hydrolytic degradation of phospholipids.[14] Moreover, the preparation of unilamellar vesicles using phospholipids with uniform distribution is comparatively difficult than that of multilamellar ones.[9] Therefore, the utility of phospholipid−liposomes as the drug delivery vehicle and models for biological membranes is restricted because of their lack of physical and chemical stability. Hence, it is of great importance in the field of science to develop new self-assembled vesicular systems of alternative building blocks. During the past few years, researchers have witnessed development of various new nonphospholipid vesicular aggregates composed of different polymers and surface active agents.[15−17] The applicability of micro and nanostructures of vesicular aggregates depends upon their stability, size, morphology, polydispersity, and composition. Among all vesicular systems,[15−17] the nonionic surfactant-based vesicles which are well-known as niosomes gain

Received: June 7, 2017
Accepted: October 26, 2017
Published: November 7, 2017

DOI: 10.1021/acsomega.7b00744
ACS Omega 2017, 2, 7637−7646

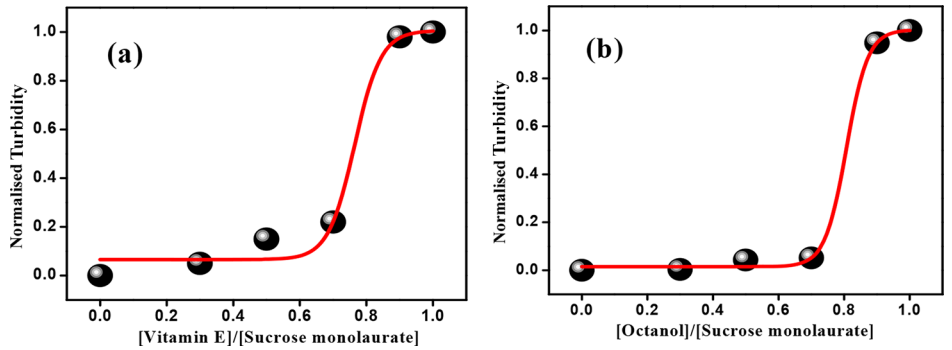

Figure 1. Variation of turbidity of (a) sucrose monolaurate−vitamin E- and (b) sucrose monolaurate−octanol-containing niosomes at different *R* values.

significant attention because of their unique features over the others. Very often, niosomes can be considered as a substitute to liposomes.[8,18−28] The nonionic surfactant is the main amphiphilic constituent of niosomes. The niosomal aggregates are more advantageous compared to liposomes because of their easy preparation procedures, high stability, and also relatively low cost of the surfactants. The low toxicity, biocompatibility, and biodegradability of niosomes increase their applicability in drug delivery. Similar to liposomes, niosomes can effectively bind hydrophobic molecules in their hydrophobic bilayer and hydrophilic molecules in their aqueous hydrophilic core, which makes them a promising candidate in the fields of drug delivery and pharmaceuticals.[29−32]

Considering the usefulness of niosomes, in this article, we have formulated a newly developed niosomal assemblies involving carbohydrate moiety containing nonionic surfactant sucrose monolaurate with vitamin E and octanol as additives. Vitamin E (α-tocopherols, α-Toc) is a fat-soluble essential vitamin with a well-known antioxidant property. It is situated in the chloroplast envelope, thylakoid membranes in green plant tissues, and also in the plastoglobuli.[33,34] It has been shown that α-Toc is involved in intercepting free radicals diffusing into the membrane from the aqueous phase.[35] In addition to the membrane protective role, other actions of vitamin E, such as enzyme activation, inhibition of cell proliferation, and so forth, have been reported.[36,37] Vitamin E influences the membrane dynamics and shows strong interactions in its effects on membrane stability during freezing. Although, there are several studies regarding effects of vitamin E on the phospholipid membranes, nothing is known about the role of vitamin E in the formation of niosomes. On the other hand, the other additive we have used is a long-chain alcohol, *n*-octanol, to formulate another class of novel niosomal aggregates. There are few studies on the effect of alkanols on the morphology of micelles and phospholipid vesicles.[38−42] It has been reported that microstructural transition of aqueous cetrimonium bromide (CTAB) micelles takes place in the presence of octanol and inorganic salt, KBr.[43] The molecular dynamics simulation study also suggests that microstructural alteration of CTAB occurs in the presence of octanol.[44]

Long-chain alcohol also has a unique effect toward membrane properties as mentioned in the literature.[39] It has been reported that the presence of octanol promotes the lipid diffusion process and also affects the phase behavior of lipids.[38] The acyl chain order/fluidity of the membrane is also affected by the presence of *n*-alkanol.[45] Therefore, the literature reports as well as the future scopes of octanol-induced morphological transitions have made us curious to investigate the role of *n*-octanol as an artificial vesicle-forming agent for a nonionic amphiphile. To the best of our knowledge, this is the first report which reveals the morphological transition of a carbohydrate-based nonionic surfactant into niosome using vitamin E and octanol as additives. The structural characterization of niosome formation is systematically monitored by turbidity, dynamic light scattering (DLS), ξ potential, NMR, and transmission electron microscopy (TEM) measurements. UV−vis spectroscopy and time-resolved anisotropy measurements of a hydrophobic probe coumarin 153 (C153) have also been carried out to monitor the dynamic changes that take place in the vitamin E/octanol−sucrose monolaurate containing niosomal formulations. Therefore, this particular study may unveil some interesting aspects toward the effect of a vitamin and octanol into the nonionic amphiphilic assembly. In addition, the cytocompatibility of these niosomal formulations have been investigated with primary chondrocyte cell lines. These vitamin E/octanol−sucrose monolaurate niosomes are utilized to entrap doxorubicin, an anticancer drug inside mammalian cells which is monitored by fluorescence microscopic images.

2. RESULTS AND DISCUSSION

2.1. Structural Characterizations of Nonionic Surfactant and Octanol- and Vitamin E-Containing Aggregates. *2.1.1. Turbidity Study.* The morphological transition of nonionic surfactant sucrose monolaurate in the presence of vitamin E or octanol is investigated through monitoring the phase behavior of various niosome formulations. Here, it is important to discuss that we have checked with alcohols having shorter chain length than *n*-octanol and found that niosome formation takes place from *n*-octanol at the experimental condition. This is supported by the optical micrographs, as shown in Figure S1 of the Supporting Information. Now, with the incorporation of vitamin E and *n*-octanol, certain visual alteration in the phase behavior is monitored. In addition, we have also measured the turbidity of various niosomal formulations by monitoring their absorbance at 600 nm. The absorbance of the individual components including the nonionic surfactant is found to be negligible at this wavelength (Figure S2, Supporting Information). Hence, the observed variations in turbidity are due to the scattering of light by the newly formed larger-sized aggregates present in solution. Actually, there are few literature studies which support the formation of different large aggregates in the presence of vitamin E derivatives[46] and also long-chain alcohols.[43] Figure

DOI: 10.1021/acsomega.7b00744
ACS Omega 2017, 2, 7637−7646

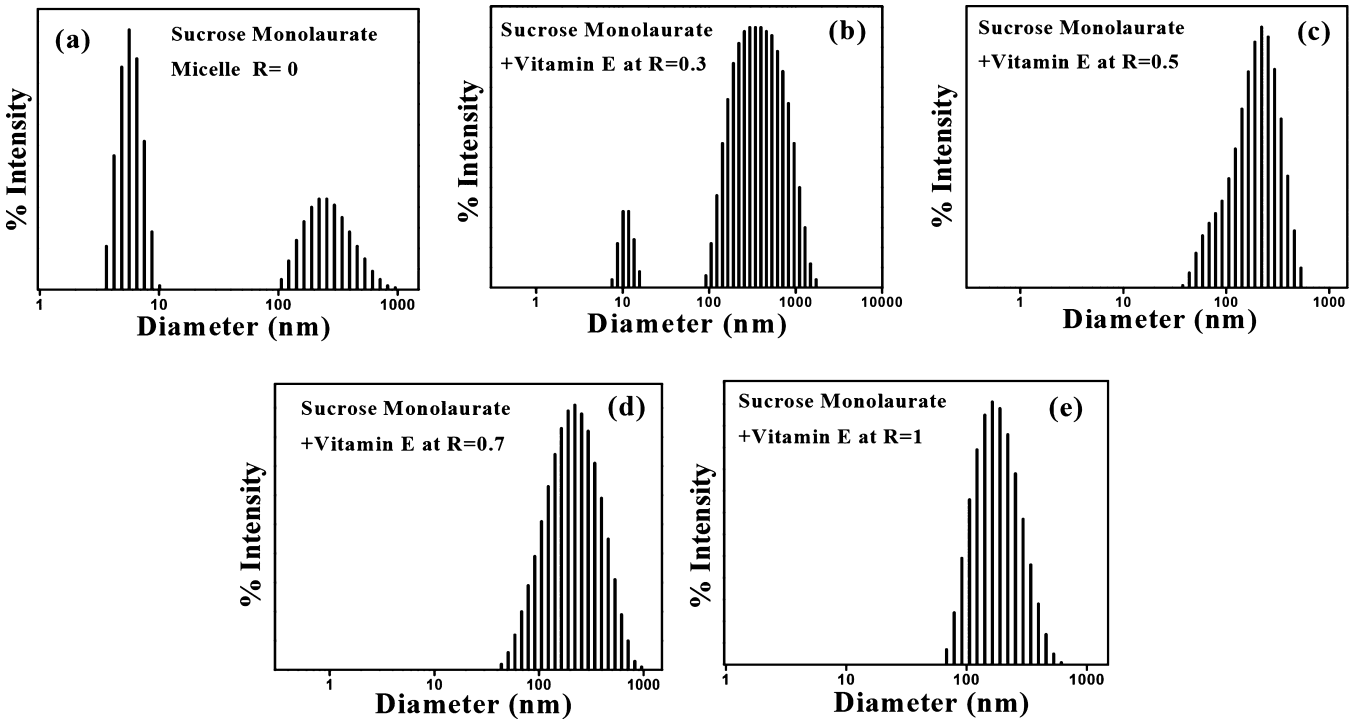

Figure 2. DLS intensity−size distribution of sucrose monolaurate−vitamin E-containing niosomes at (a) $R = 0$, (b) $R = 0.3$, (c) $R = 0.5$, (d) $R = 0.7$, and (e) $R = 1$.

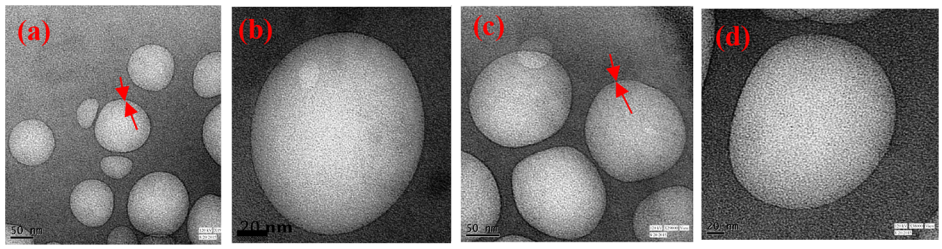

Figure 3. TEM images of unilamellar niosomes of sucrose monolaurate−vitamin E (a,b) and sucrose monolaurate−octanol (c,d) at $R = 1$.

1a,b describes the variation of turbidity of solution mixtures as a function of vitamin E and octanol concentration, respectively. The sharp enhancement in turbidity of the solution mixtures indicates the formation of larger niosomal aggregates.

2.1.2. DLS Measurements. To unravel the microstructural transition of the sucrose monolaurate micellar assembly into niosomes with increasing vitamin E or octanol concentration, DLS measurement has been performed. Figures 2 and S3, (Supporting Information) represent the intensity−size distribution profiles of vitamin E- and octanol-containing niosomal aggregates, respectively. We maintain the concentration of sucrose monolaurate at 10 mM which is well above its critical micelle concentration as reported in the literature.[47] At this particular concentration, sucrose monolaurate aggregates as micelles, and the average diameter of the micellar aggregates lies in the range of ∼5 nm. Interestingly, in the DLS histogram of the sucrose monolaurate micelle, there is an intense peak that appears in the larger diameter region, the reason of which is discussed in the latter section. Briefly, DLS is an intensity-based measurement technique, and the scattering light intensity ($I_{scatter}$) is directly proportional to the sixth power of the particle diameter (r^6). Therefore, intensity−size distribution DLS profiles are very much sensitive toward the presence of large particles in the solution, and even if a trace amount of large particles are present in the solution, they will be reflected in the DLS profile. However, a remarkable change in the intensity−size distribution plots is monitored with the gradual increment of vitamin E and octanol concentrations. The gradual addition of vitamin E and octanol leads to the formation of niosomes having a diameter of ∼150−350 nm. Several groups also reported similar types of size distribution profiles for different cationic surfactants and cholesterol-containing vesicular aggregates which also strongly support our results.[28,48] The DLS size distribution plots obtained are monomodal, having a low polydispersity index which suggests that spherical aggregates are present in the solution. Therefore, from the DLS measurement, we can successfully conclude that incorporation of vitamin E and octanol in the sucrose monolaurate micelle leads to micelle-to-niosome transition.

2.1.3. TEM Measurements. TEM is the direct evidence for the formation of niosomes with a distinct bilayer. The TEM images of vitamin E- and octanol-containing niosomes are depicted in Figure 3a,b and 3c,d, respectively. The size of the vesicles obtained from the TEM measurement is smaller than that obtained from the scattering measurement. TEM is the size measurement tool which depends mainly on the number of the particles, whereas DLS is usually an intensity-based measurement technique. Therefore, DLS is very sensitive to large

DOI: 10.1021/acsomega.7b00744
ACS Omega 2017, 2, 7637−7646

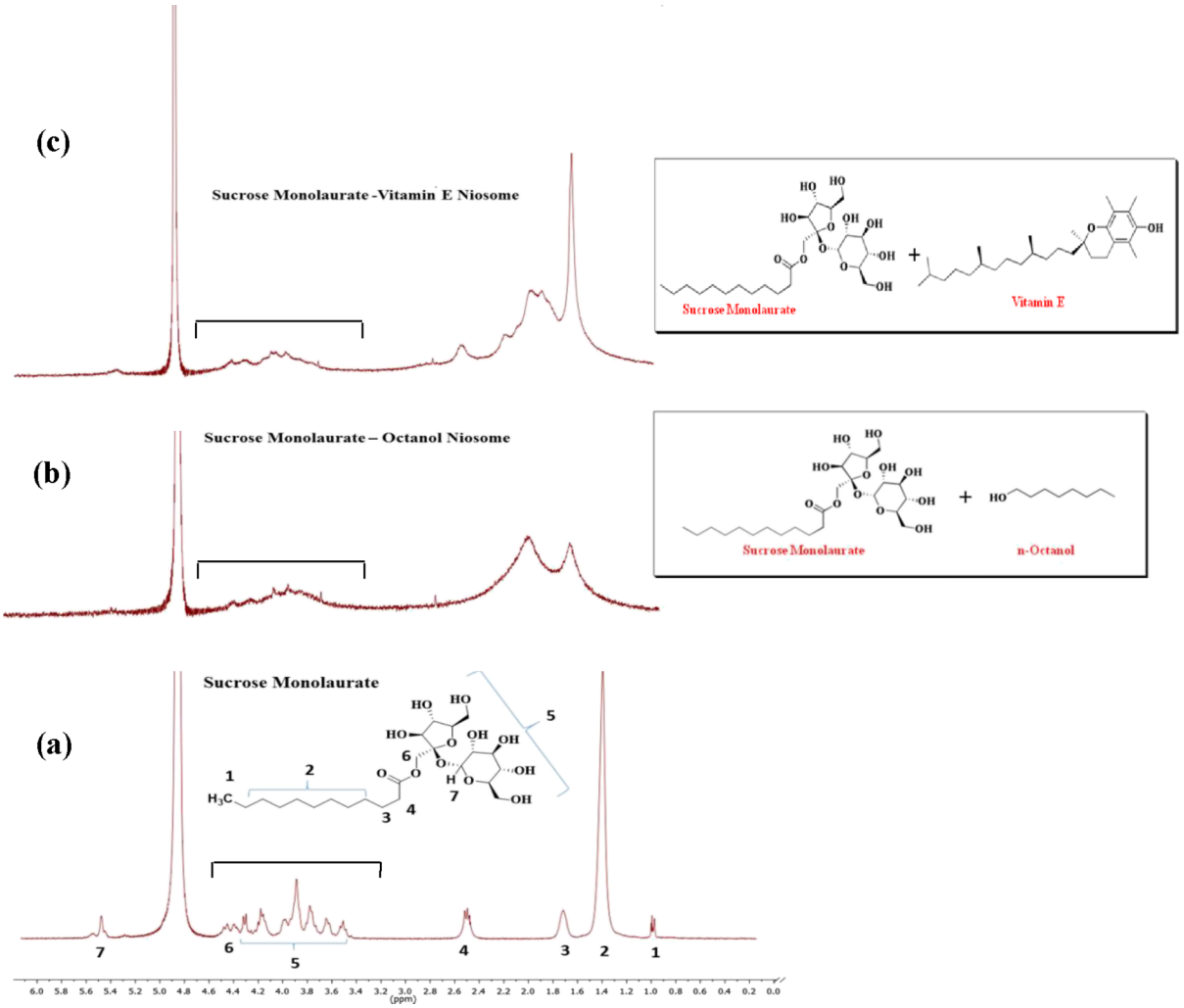

Figure 4. ^{1}H NMR spectra of (a) sucrose monolaurate micelle, (b) sucrose monolaurate−octanol niosome, and (c) sucrose monolaurate−vitamin E niosome. All spectra use the D_2O solvent signal at ∼4.8 ppm as a reference. The numberings correspond to the protons of respective groups of sucrose monolaurate as shown in the figure. The third bracated portions show the broadening of alkyl chain protons of sucrose monolaurate due to the formation of niosomes.

particles (according to Rayleigh's approximation, intensity is proportional to r^6), and because TEM is a number-based technique, it will show stronger emphasis of the smallest components in the size distribution.[49]

From the TEM images, it is revealed that the average size of the spherical unilamellar niosomes is ∼70−100 nm, although some niosomes having a smaller size distribution also exist. Therefore, we have successfully demonstrated that individually vitamin E and *n*-octanol can lead to the formation of niosomes in the aqueous solution of a carbohydrate-based nonionic surfactant, sucrose monolaurate.

2.1.4. NMR Studies. Further, ^{1}H NMR measurement has been applied to understand the microstructural alterations of sucrose monolaurate into niosomes upon interaction with vitamin E and octanol. The ^{1}H NMR technique helps to interpret the synergistic interaction between the nonionic micelle sucrose monolaurate and the two individual additives (vitamin E and octanol) involved in the formation of various niosomal formulations. From Figure 4, it is evident that the NMR peaks corresponding to the protons of the alkyl chain of sucrose monolaurate are considerably broadened in the niosomal solutions composed of vitamin E and octanol.

It is also monitored that the triplet peak responsible for the protons (H4) adjacent to the carbonyl carbon is merged into a single broad peak as micelles are transformed into niosomes upon interaction with vitamin E and octanol. Moreover, all protons attached to the carbohydrate backbone are also broadened significantly. The formation of rigid self-organized protocell membranes, such as niosomes, renders the hindered movement and shorter relaxation times of the nuclei which is manifested in the certain broadening of peaks in the NMR spectra.[50] By applying the ^{1}H NMR relaxation methodology, Villeneuve et al.[51] investigated the morphological transformation of the aqueous mixture of common cationic and anionic surfactants. Their study revealed that the liquid-crystal-like nature in the vesicle interior, various curvatures of the bilayered vesicles, and the induced polydispersity of the vesicular aggregates are responsible for the broadening of the NMR peaks in vesicular solutions.

2.1.5. Zeta Potential (ξ) Measurements. The surface charge of the vitamin E- and octanol-containing niosomes is determined by zeta potential (ξ) measurement. The difference of electrical potential between the dispersion medium and the stationary layer that exists over the surface of aggregates is

DOI: 10.1021/acsomega.7b00744
ACS Omega 2017, 2, 7637−7646

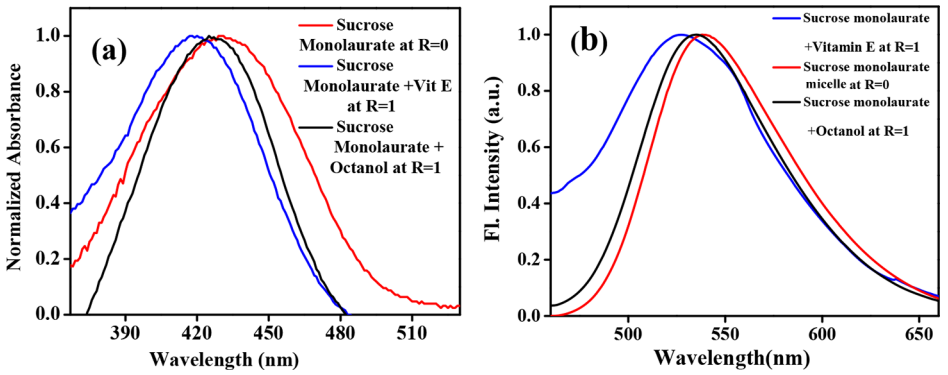

Figure 5. Variation in (a) UV−vis absorption and (b) emission spectra of C153 in sucrose monolaurate-, sucrose monolaurate−vitamin E-, and sucrose monolaurate−octanol-containing niosomes at R = 1.

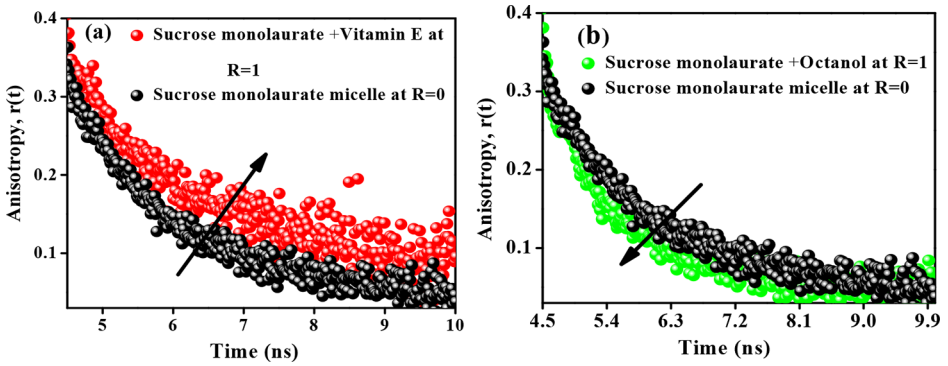

Figure 6. Variation in time-resolved anisotropy of C153 in (a) sucrose monolaurate−vitamin E- and (b) sucrose monolaurate−octanol-containing niosome at R = 1.

termed as ξ potential. On account of the thermal motion of water molecules, the dispersion medium is extended from the surface of the aggregates.

The micellar surface of sucrose monolaurate is negatively charged, and the ξ potential alters sharply with the addition of vitamin E and octanol into the micellar solution, that is, the ξ value becomes more negative in vitamin E and octanol-forming niosomal assemblies at R = 0.3. Moreover, the numerical value of ξ increases slightly upon further increase in vitamin E and octanol content. Vitamin E or octanol molecules are neutral, and their incorporation results in transformation of smaller micellar aggregates into larger niosomes. Moreover, the hydrogen bonding interaction is taking place between the head group region of sucrose monolaurate and the hydroxyl groups of the vitamin E and octanol molecules. Hence, a greater number of surfactant molecules are densely packed in vesicular aggregates which results in a significant enhancement of the surface charge of niosomes (Figure S4, Supporting Information).

2.1.6. Steady-State Anisotropy Studies. The micelle-to-niosome transitions of the sucrose monolaurate solutions are further investigated by the steady state fluorescence anisotropy measurements. The steady-state fluorescence anisotropy of both sucrose monolaurate−vitamin E and sucrose monolaurate−octanol solutions with the increasing R value is measured using 1,6-diphenyl-1,3,5-hexatriene (DPH) as a fluorescent probe (Figure S5, Supporting Information). DPH is a well-known membrane-bound probe which is widely used to get insight into rigidity of the membrane.[52] For the sucrose monolaurate−vitamin E niosome system, the anisotropy values are increased as micelles are gradually transformed into niosomes upon increasing the concentration of vitamin E. This observation clearly indicates that the surrounding microenvironment of DPH in sucrose monolaurate micelles is less rigid compared to that in niosomes. The higher the value of anisotropy is, the higher will be the extent of incorporation of the probe into the rigid and confined microenvironments of the niosome bilayer taking place. However, for the sucrose monolaurate−octanol niosomes, the exactly reverse trend in steady state anisotropy is monitored with the increasing concentration of octanol. The reduction of anisotropy values indicates that the DPH molecule is experiencing less rigid and confined microenvironment in sucrose monolaurate−octanol niosome compared to that in micellar environment of sucrose monolaurate. The detailed discussions of the different microenvironments of these niosomes have been provided in the time-resolved anisotropy measurements section.

2.1.7. Photophysical Investigation of a Hydrophobic Molecule in Sucrose Monolaurate−Vitamin E/Octanol-Containing Niosomes. 2.1.7.1. Steady-State Measurements. The UV−vis absorption and steady-state emission measurements of C153 have been monitored in sucrose monolaurate-containing self-assemblies to investigate the alteration in microenvironments surrounding the probe molecule as a result of interaction with vitamin E and octanol.

The normalized absorption spectra of C153 in the sucrose monolaurate micelle, sucrose monolaurate−octanol, and sucrose monolaurate−vitamin E niosomes are shown in Figure 5a. The absorption maximum of C153 in sucrose monolaurate is 431 nm. When vitamin E is incorporated into the carbohydrate-based nonionic surfactant, the absorption maximum is 10 nm blue-shifted. On the other hand, in octanol-

DOI: 10.1021/acsomega.7b00744
ACS Omega 2017, 2, 7637−7646

containing niosomes, the extent of blue shift is less than vitamin E-containing niosomes. The absorption maximum is blue-shifted by 4 nm in sucrose monolaurate−octanol niosomes. The emission maximum of C153 in sucrose monolaurate comes around 538 nm. In sucrose monolaurate−vitamin E and sucrose monolaurate−octanol niosomes, the emission maxima of C153 are blue-shifted to ∼535 and ∼529 nm, respectively (Figure 5b). This blue-shifted absorption and emission maxima indicate the inclusion of the hydrophobic probe C153 into the hydrophobic bilayer of niosomes composed of vitamin E and octanol. Moreover, the greater extent of blue shifting is the indication of higher hydrophobicity of the vitamin E−sucrose monolaurate system compared to that of the octanol−sucrose monolaurate niosome. Moreover, we have also checked the excitation spectra of all sets of solutions, and the excitation spectra resemble the absorption spectra which indicate the purity of the samples (Figure S6, Supporting Information).

2.1.7.2. Time-Resolved Anisotropy Measurements. The solubilization site of the probe molecule and its dynamics in self-organized systems can be regulated by a structural aspect of different self-assemblies. Therefore, we have monitored the rotational motion of the C153 molecule in various systems to gain further insight into the microenvironment of the niosomes.

The anisotropy decays of C153 during the micelle−niosome transition in different systems are depicted in Figure 6a,b. In bulk water, the C153 molecule shows a single exponential decay profile having a rotational time constant of ∼100 ps.[52] However, in micellar and niosomal aggregates, the anisotropy decays become biexponential. The corresponding anisotropy decay parameters are provided in Table 1.

Table 1. Decay Parameters of Rotational Relaxation of C153 in Sucrose Monolaurate−Vitamin E and (b) Sucrose Monolaurate−Octanol-Containing Niosomes at R = 1 (λ_{ex} = 440 nm)

systems	a_1	τ_1 (ns)	a_2	τ_2 (ns)	$\langle\tau_r\rangle^a$ (ns)
sucrose monolaurate	0.45	0.75	0.55	3.74	2.39
vitamin E niosome at R = 1	0.40	0.35	0.60	4.72	2.97
octanol niosome at R = 1	0.57	0.11	0.43	2.04	0.94

[a]Experimental error of ±5%.

The average reorientation time of C153 in the sucrose monolaurate micelle is ∼2.39 ns. The rotational motion of C153 is hindered as the concentration of vitamin E increases in the aqueous solutions of sucrose monolaurate. The average rotational time constant of C153 in vitamin E-containing niosome is 2.97 ns. This ensures that C153 is incorporated into the confined and restricted microenvironments of the niosome because of the morphological transformation of sucrose monolaurate micelles into niosome upon interaction with vitamin E. The faster rotational motion of hydrophobic C153 can be justified by the location and arrangement of the octanol molecule inside the sucrose monolaurate micellar assemblies. The nonpolar moiety of octanol is not as long as the hydrocarbon chains of sucrose monolaurate. This may result in some void spaces between the chains in the bilayer interior of the octanol-forming niosomes. This type of void formation is reported for the lipid vesicles in the presence of small amphiphilic molecules.[39]

Therefore, the probe molecules may rotate more freely in the octanol-containing niosomes and hence, there is a decrease in the average rotational relaxation time. Therefore, the micro-environments of the niosomes composed of vitamin E and octanol are quite different from each other.

The possible picture of the molecular arrangement has been given in the following scheme where we can see the difference between molecular arrangements of the two additives in these two niosomal systems. There are reports of cholesterol-induced niosome formation where the hydroxyl group of cholesterol forms hydrogen bonding with the carbonyl group of Tween 80 and governs niosome formation.[29] Similarly, here, the hydrogen bonding between hydroxyl moiety of vitamin E/ octanol and the carbonyl group of sucrose monolaurate governs the formation of the niosome. As discussed earlier, the hydrocarbon chain of octanol is not as long as the nonpolar moiety of sucrose monolaurate. This may result in some void spaces between the chains in the bilayer of the sucrose monolaurate−octanol niosome (Scheme 1).

The Scheme 1 represents the pictorial representation of the molecular arrangement of vitamin E and octanol in their respective niosomes.

However, for vitamin E, there is no such possibility of void space formation as the nonpolar hydrocarbon region of vitamin E has almost similar length with that of sucrose monolaurate. Therefore, the difference in microenvironments of the niosomes composed of vitamin E and octanol can be represented as given in Scheme 1.

2.1.7.3. Cytotoxicity Determined by MTT Assay. To exploit the superior doxorubicin encapsulation ability of vitamin E/ octanol−sucrose monolaurate niosomes, one of the prereq-uisites is to ensure the cytocompatibility of the niosomes. The cytocompatibility of the initial micelles and niosomes is studied against mammalian cells (primary chondrocyte cells) by MTT assay. After 1 h of incubation, around 97% of the cells remain healthy and alive in vitamin E−sucrose monolaurate niosomes (Figure 7a). After 3 h of incubation, the absorbance value enhances for vitamin E−sucrose monolaurate, which indicates that the normal cell growth is not inhibited in the presence of this particular niosome system (Figure 7b). However, the absorbance value obtained for octanol−sucrose monolaurate

Scheme 1. Pictorial Representation of the Molecular Arrangement of Vitamin E and Octanol in Their Respective Niosomes

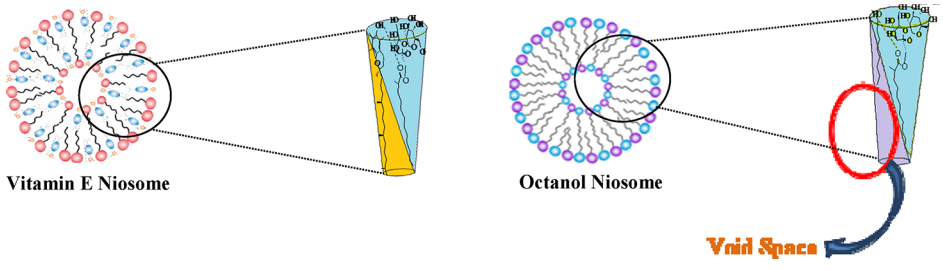

DOI: 10.1021/acsomega.7b00744
ACS Omega 2017, 2, 7637−7646

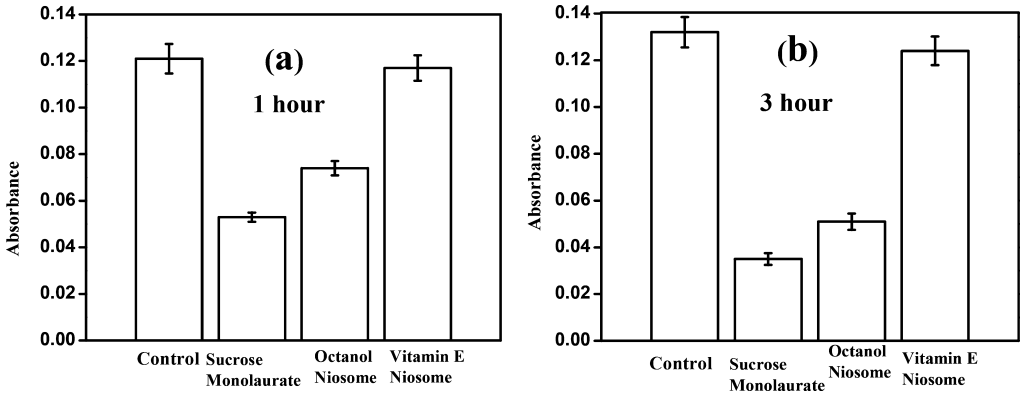

Figure 7. Cytotoxicity study of the niosomes composed of vitamin E and octanol by MTT assay at (a) 1 and (b) 3 h time interval.

niosomes is less compared to that obtained for vitamin E–sucrose monolaurate niosomes in both time scales. Hence, the vitamin E-containing niosomal system is almost nontoxic for the cells compared to that of the octanol-forming niosomes. This may be due to the inherent toxicity of the alcohols toward the cell membrane.[53] Moreover, the absorbance value is further reduced for the sucrose monolaurate micelle which indicates that the cytotoxicity of these micelles is higher than the vitamin E/octanol–sucrose monolaurate niosomes.

In the presence of the sucrose monolaurate system, only 44% cells remain alive for the 1 h incubation period. After 3 h, it is further reduced to 27% which indicates greater cytotoxicity of the sucrose monolaurate micelle compared to that of the niosomes. This is in correlation with the previous literature report of the membrane lysis by nonionic surfactant-forming amphiphiles.[54] Thus, vitamin E–sucrose monolaurate niosomes show substantial cell viability compared to the octanol–sucrose monolaurate niosomes and sucrose monolaurate micelles.

2.1.7.4. Cellular Internalization. Doxorubicin-loaded vitamin E/octanol–sucrose monolaurate niosomes are incubated with primary chondrocyte cells for 3 h. These mammalian cells incubated with niosomes are found to be in natural shape after the incubation period which indicates the healthy morphology of the cells (Figure 8). Importantly, after 3 h of incubation, the red fluorescence images of the cells confirm the successful internalization of doxorubicin within the primary chondrocyte cells. However, the cells remain well-shaped in vitamin E–sucrose monolaurate niosomes compared to that in octanol–sucrose monolaurate niosomes. Moreover, in the presence of sucrose monolaurate incubation, the cell morphology alters and less spread on the surface. Actually, it is reported that micelle-forming surfactants induce disordering in cell membranes that causes lysis of the membrane which has also been observed in life cells.[54,55] However, there are reports of using vesicular systems for drug delivery purposes in living systems.[8,11,29−32] Moreover, cholesterol-based vesicles have been utilized for cellular transportation. It has been reported that the cholesterol-derived vesicles are nontoxic for cells, and the cellular membrane remains intact in the presence of these vesicles.[29,30]

Our investigation reveals that the cell count is less in micelles compared to the niosome-incubated cells, which is also well-correlated with the MTT assay. Hence, more number of cells are affected in the case of sucrose monolaurate micelle incubation. However, from the cell imaging and MTT assay, it is also revealed that the vitamin E-forming niosomes are cytocompatible and cells are not at all affected. Therefore, these

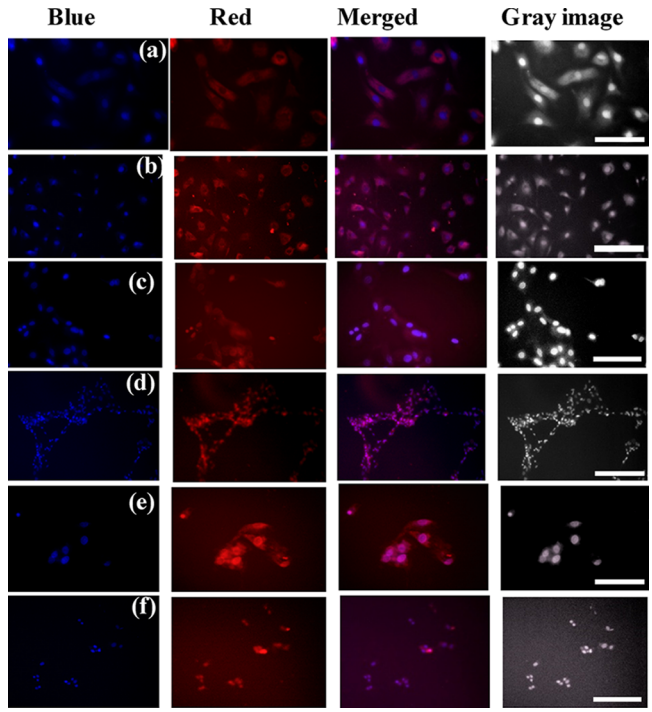

Figure 8. Fluorescence microscopic images and gray images of primary chondrocyte cells incubated with doxorubicin-loaded (a,b) vitamin E–sucrose monolaurate niosomes, (c,d) octanol–sucrose monolaurate niosomes, and (e,f) sucrose-monolaurate micelles for 3 h at (a,c,e) 20× magnification and (b,d,f) 10× magnification. Dox shown in red, 4′,6-diamidino-2-phenylindole (DAPI)-stained cell nuclei shown in blue. The 100 and 50 μm scale bars represent 10× magnification and 20× magnification, respectively.

sucrose monolaurate niosomes, particularly the vitamin E–sucrose monolaurate niosomes, hold immense potential to be utilized as a cellular transporter.

3. CONCLUSION

In summary, we have developed a novel class of niosomes composed of a carbohydrate-based amphiphile sucrose monolaurate, where vitamin E and a long-chain alcohol octanol are the other components. Detailed characterization of these niosomes has been carried out through DLS, TEM, turbidity, ξ potential, and NMR measurements. In addition, the micro-environments of these two different niosomes have been investigated through monitoring the rotational motion of a hydrophobic probe using steady-state and time-resolved

DOI: 10.1021/acsomega.7b00744
ACS Omega 2017, 2, 7637−7646

Scheme 2. Structures of Sucrose Monolaurate, α-Tocopherol, DPH, C153, and *n*-Octanol

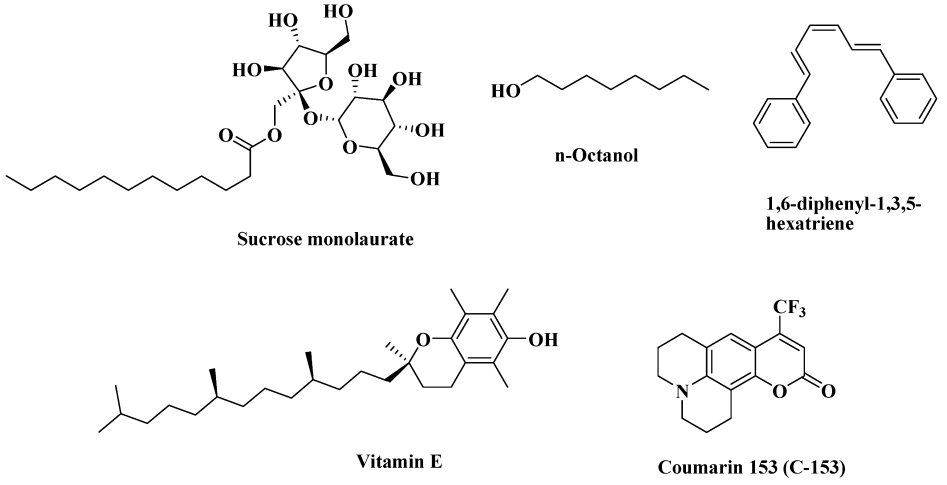

anisotropy measurements. In both these steady-state and time-resolved anisotropy measurements, it has been found that the bilayer of vitamin E-forming niosomes is more compact and rigid compared to the micelle; however, the opposite trend is observed for the octanol-based niosomal formulation. We have explained this contrasting photophysical behavior in terms of the difference in alkyl chain lengths of niosome-forming components, where shorter alkyl chain of octanol results in some void spaces between the chains in the bilayer of sucrose monolaurate−octanol niosomes. More importantly, this newly developed novel class of niosomes has lesser cytotoxicity compared to that of the neat sucrose monolaurate micelle. The ability to entrap dye/probe molecules by these niosomes is used to entrap doxorubicin inside the mammalian primary chondrocyte cells. Moreover, the cytotoxicity of the sucrose monolaurate−vitamin E niosome is lesser compared to the sucrose monolaurate−octanol niosome and sucrose monolaurate micelle itself. Therefore, the vitamin E-containing niosomal formulation has potential importance and might be used for further applications in the pharmaceutical field.

4. EXPERIMENTAL SECTION

4.1. Materials. Sucrose monolaurate, α-tocopherol, and DPH were purchased from Sigma-Aldrich. C153 was obtained from Exciton and used as received. Triply distilled Milli-Q water was used for the solution preparation. The concentration of sucrose monolaurate was kept 10 mM for all measurements. All experiments were performed at 298 K temperature.

The structures of sucrose monolaurate, α-tocopherol, DPH, C153, and *n*-octanol are given in Scheme 2.

4.2. Instrumentations. *4.2.1. Steady-State Measurements.* The steady-state absorption spectra of C153 were monitored using a Shimadzu spectrophotometer (model number UV-2450), and the emission spectra was collected using a Hitachi (model number F−7000) spectrofluorimeter.

4.2.2. Time-Resolved Fluorescence Anisotropy Measurements. For time-resolved anisotropy measurements, we have used the picosecond time-correlated single photon counting (TCSPC) setup. In our earlier publication, the detailed description of the TCSPC setup was provided.[28] Basically, a picosecond diode laser (IBH, UK, NanoLED) of 440 nm was used as an excitation source. The Hamamatsu microchannel plate photomultiplier tube (3809U) was used as a detector.

The details regarding instrumentation, solution preparation, turbidity measurement, DLS (Malvern Nano ZS instrument), ξ potential, TEM, and NMR measurement are given in the Supporting Information.

4.3. Cell Culture Using Primary Chondrocyte Cells. Primary chondrocyte cells were isolated from rabbit ear according to the previously described method with some modifications.[56] Rabbits were euthanized, and ear samples were collected thereafter. The samples were initially washed with povidone iodine solution, and skin layers on ear samples were peeled off. The tissue was thereafter diced into small pieces and incubated in pronase solution for 30 min followed by 0.3% collagenase II solution (Gibco) on a shaker incubator at 200 rpm for 4 h at 37 °C. The digested tissues were passed through 100 μm cell strainers, and filtered cell suspension was neutralized and washed. Cells were then pelleted by centrifugation and grown in Dulbecco's modified Eagle's medium supplemented with 10% fetal bovine serum, 100 mg/mL amphotericin B, and 100 units/mL penicillin. After reaching confluency, the cells were passaged at a ratio of 1:4 and used in these studies.

4.3.1. Cell Cytotoxicity and Viability Studies. 4.3.1.1. MTT Assay. Cellular cytotoxicity was measured by MTT [3-(4,5-dimethylthiazol-2-yl)-2,5-diphenyltetrazolium bromide] assay. In a 12-well plate, 10^4 cells/well were seeded and incubated at 37 °C for 24 h, followed by the addition of samples at a concentration of 10 mM. After 1 and 3 h of incubation with samples, the wells were washed with phosphate-buffered saline (PBS) and incubated in 0.5 mg/mL MTT solution at 37 °C for 4 h. To dissolve the formazan crystals thus formed, dimethyl sulfoxide was added and stirred, and absorbance was recorded at 595 nm on a microplate reader on the plate screen (RMS, Chandigarh, India).[57]

4.3.1.2. Doxorubicin Loading and Cellular Studies. Dox loading was performed by incubating niosomes in 1 mg/mL of Dox solution overnight. Because of the hydrophilic nature of Dox, it preferentially accumulates in the inner aqueous core of the niosomes. After preparation, the Dox-loaded niosome aqueous suspension was stored in dark atmosphere at 4 °C and later used for further fluorescence experiments in cells.

For fluorescence studies, in a 12-well plate, 10^4 cells/well were seeded and incubated at 37 °C for 24 h, followed by the addition of samples at a concentration of 10 mM. After 3 h of incubation with samples, the wells were washed with PBS and

DOI: 10.1021/acsomega.7b00744
ACS Omega 2017, 2, 7637−7646

stained using DAPI (Thermo Fisher Scientific) following the manufacturer's protocol.[57] An Axio Observer Z1 microscope (Carl Zeiss, Germany) was used for capturing images.

■ ASSOCIATED CONTENT

Supporting Information

The Supporting Information is available free of charge on the ACS Publications website at DOI: 10.1021/acsomega.7b00744.

The detailed descriptions of the instrumental section, DLS plot, steady-state anisotropy plots, and ξ potential plot have been provided in the Supporting Information (PDF)

■ AUTHOR INFORMATION

Corresponding Author

*E-mail: nilmoni@chem.iitkgp.ernet.in. Fax: 91-3222-255303.

ORCID

Santanu Dhara: 0000-0001-8599-569X

Nilmoni Sarkar: 0000-0002-8714-0000

Notes

The authors declare no competing financial interest.

■ ACKNOWLEDGMENTS

N.S. gratefully acknowledges SERB, Department of Science and Technology (DST), Government of India for providing generous research grant. A.R., A.P., and P.P. are thankful to CSIR for research fellowships.

■ REFERENCES

(1) Dong, R.; Hao, J. Complex Fluids of Poly(oxyethylene) Monoalkyl Ether Nonionic Surfactants. *Chem. Rev.* **2010**, *110*, 4978−5022.

(2) Dong, R.; Liu, W.; Hao, J. Soft Vesicles in the Synthesis of Hard Materials. *Acc. Chem. Res.* **2012**, *45*, 504−513.

(3) Hotz, J.; Meier, W. Vesicle-Templated Polymer Hollow Spheres. *Langmuir* **1998**, *14*, 1031−1036.

(4) Pileni, M.-P. The Role of Soft Colloidal Templates in Controlling the Size and Shape of Inorganic Nanocrystals. *Nat. Mater.* **2003**, *2*, 145−150.

(5) Bangham, A. D. Membrane Models with Phospholipids. *Prog. Biophys. Mol. Biol.* **1968**, *18*, 29−95.

(6) Akbarzadeh, A.; Rezaei-Sadabady, R.; Davaran, S.; Joo, S. W.; Zarghami, N.; Hanifehpour, Y.; Samiei, M.; Kouhi, M.; Nejati-Koshki, K. Liposome: Classification, Preparation, and Applications. *Nanoscale Res. Lett.* **2013**, *8*, 102.

(7) György, B.; Hung, M. E.; Breakefield, X. O.; Leonard, J. N. Therapeutic Applications of Extracellular Vesicles: Clinical Promise and Open Questions. *Annu. Rev. Pharmacol. Toxicol.* **2015**, *55*, 439−464.

(8) Kumar, G. P.; Rajeshwarrao, P. Nonionic Surfactant Vesicular Systems for Effective Drug Delivery—an Overview. *Acta Pharm. Sin. B* **2011**, *1*, 208−219.

(9) Szoka, F.; Papahadjopoulos, D. Comparative Properties and Methods of Preparation of Lipid Vesicles (Liposomes). *Annu. Rev. Biophys. Bioeng.* **1980**, *9*, 467−508.

(10) Song, A.; Jia, X.; Teng, M.; Hao, J. Ca^{2+}- and Ba^{2+}-Ligand Coordinated Unilamellar, Multilamellar, and Oligovesicular Vesicles. *Chem.—Eur. J.* **2007**, *13*, 496−501.

(11) Lian, T.; Ho, R. J. Y. Trends and Developments in Liposome Drug Delivery Systems. *J. Pharm. Sci.* **2001**, *90*, 667−680.

(12) Guo, X.; Szoka, F. C., Jr. Chemical Approaches to Triggerable Lipid Vesicles for Drug and Gene Delivery. *Acc. Chem. Res.* **2003**, *36*, 335−341.

(13) Medvedeva, D. A.; Maslov, M. A.; Serikov, R. N.; Morozova, N. G.; Serebrenikova, G. A.; Sheglov, D. V.; Latyshev, A. V.; Vlassov, V. V.; Zenkova, M. A. Novel Cholesterol-Based Cationic Lipids for Gene Delivery. *J. Med. Chem.* **2009**, *52*, 6558−6568.

(14) Minami, H.; Inoue, T.; Shimozawa, R. Kinetics of Divalent Cation-Induced and pH-Induced Aggregation of Dimyristoylphosphatidylserine Vesicles. *J. Colloid Interface Sci.* **1994**, *164*, 9−15.

(15) Moniruzzaman, M.; Tahara, Y.; Tamura, M.; Kamiya, N.; Goto, M. Ionic Liquid-Assisted Transdermal Delivery of Sparingly Soluble Drugs. *Chem. Commun.* **2010**, *46*, 1452−1454.

(16) Stano, P.; Wehrli, E.; Luisi, P. L. Insights into the self-reproduction of oleate vesicles. *J. Phys.: Condens. Matter* **2006**, *18*, S2231−S2238.

(17) Stano, P.; Luisi, P. L. Achievements and open questions in the self-reproduction of vesicles and synthetic minimal cells. *Chem. Commun.* **2010**, *46*, 3639−3653.

(18) Han, W.; Wang, S.; Liang, R.; Wang, L.; Chen, M.; Li, H.; Wang, Y. Non-ionic surfactant vesicles simultaneously enhance antitumor activity and reduce the toxicity of cantharidin. *Int. J. Nanomed.* **2013**, *8*, 2187−2196.

(19) Tanner, P.; Baumann, P.; Enea, R.; Onaca, O.; Palivan, C.; Meier, W. Polymeric Vesicles: From Drug Carriers to Nanoreactors and Artificial Organelles. *Acc. Chem. Res.* **2011**, *44*, 1039−1049.

(20) Manosroi, A.; Wongtrakul, P.; Manosroi, J.; Sakai, H.; Sugawara, F.; Yuasa, M.; Abe, M. Characterization of Vesicles Prepared with Various Non-Ionic Surfactants Mixed with Cholesterol. *Colloids Surf., B* **2003**, *30*, 129−138.

(21) Schillén, K.; Bryskhe, K.; Mel'nikova, Y. S. Vesicles Formed from a Poly(ethylene Oxide)−Poly(propylene Oxide)−Poly(ethylene Oxide) Triblock Copolymer in Dilute Aqueous Solution. *Macromolecules* **1999**, *32*, 6885−6888.

(22) Ghatak, C.; Rao, V. G.; Ghosh, S.; Mandal, S.; Sarkar, N. Solvation Dynamics and Rotational Relaxation Study inside Niosome, A Nonionic Innocuous Poly(ethylene Glycol)-Based Surfactant Assembly: An Excitation Wavelength Dependent Experiment. *J. Phys. Chem. B* **2011**, *115*, 12514−12520.

(23) Mandal, S.; Rao, V. G.; Ghatak, C.; Pramanik, R.; Sarkar, S.; Sarkar, N. Photophysics and Photodynamics of 1′-Hydroxy-2′-acetonaphthone (HAN) in Micelles and Nonionic Surfactants Forming Vesicles: A Comparative Study of Different Microenvironments of Surfactant Assemblies. *J. Phys. Chem. B* **2011**, *115*, 12108−12119.

(24) Kato, K.; Walde, P.; Koine, N.; Ichikawa, S.; Ishikawa, T.; Nagahama, R.; Ishihara, T.; Tsujii, T.; Shudou, M.; Omokawa, Y.; Kuroiwa, T. Temperature-Sensitive Nonionic Vesicles Prepared from Span 80 (Sorbitan Monooleate). *Langmuir* **2008**, *24*, 10762−10770.

(25) Ghatak, C.; Rao, V. G.; Mandal, S.; Sarkar, N. Photoinduced electron transfer between various coumarin analogues and N,N-dimethylaniline inside niosome, a nonionic innocuous polyethylene glycol-based surfactant assembly. *Phys. Chem. Chem. Phys.* **2012**, *14*, 8925−8935.

(26) Paecharoenchai, O.; Niyomtham, N.; Leksantikul, L.; Ngawhirunpat, T.; Rojanarata, T.; Yingyongnarongkul, B.-e.; Opanasopit, P. Nonionic Surfactant Vesicles Composed of Novel Spermine-Derivative Cationic Lipids as an Effective Gene Carrier In Vitro. *AAPS PharmSciTech* **2014**, *15*, 722−730.

(27) Ghosh, S.; Kuchlyan, J.; Banik, D.; Kundu, N.; Roy, A.; Banerjee, C.; Sarkar, N. Organic Additive, 5-Methyl Salicylic Acid, Induces Spontaneous Structural Transformation of Aqueous Pluronic Triblock Copolymer Solution: A Spectroscopic Investigation of Interaction of Curcumin with Pluronic Micellar and Vesicular Aggregates. *J. Phys. Chem. B* **2014**, *118*, 11437−11448.

(28) Mandal, S.; Banerjee, C.; Ghosh, S.; Kuchlyan, J.; Sarkar, N. Modulation of the Photophysical Properties of Curcumin in Nonionic Surfactant (Tween-20) Forming Micelles and Niosomes: A Comparative Study of Different Microenvironments. *J. Phys. Chem. B* **2013**, *117*, 6957−6968.

(29) Sharma, V.; Anandhakumar, S.; Sasidharan, M. Self-degrading niosomes for encapsulation of hydrophilic and hydrophobic drugs: An efficient carrier for cancer multi-drug delivery. *Mater. Sci. Eng., C* **2015**, *56*, 393−400.

DOI: 10.1021/acsomega.7b00744
ACS Omega 2017, 2, 7637−7646

(30) Moghassemi, S.; Hadjizadeh, A. Nano-niosomes as nanoscale drug delivery systems: An illustrated review. *J. Controlled Release* **2014**, *185*, 22−36.
(31) Das, M. K.; Kumar, R. Development of Curcumin nano-niosomes for skin cancer chemoprevention. *Int. J. ChemTech Res.* **2015**, *7*, 747−754.
(32) Liu, T.; Guo, R. Preparation of a Highly Stable Niosome and Its Hydrotrope-Solubilization Action to Drugs. *Langmuir* **2005**, *21*, 11034−11039.
(33) Vidi, P.-A.; Kanwischer, M.; Baginsky, S.; Austin, J. R.; Csucs, G.; Dörmann, P.; Kessler, F.; Bréhélin, C. Tocopherol cyclase (VTE1) localization and vitamin E accumulation in chloroplast plastoglobule lipoprotein particles. *J. Biol. Chem.* **2006**, *281*, 11225−11234.
(34) Matringe, M.; Ksas, B.; Rey, P.; Havaux, M. Tocotrienols, the unsaturated forms of vitamin E, can function as antioxidants and lipid protectors in tobacco leaves. *Plant Physiol.* **2008**, *147*, 764−778.
(35) Afri, M.; Ehrenberg, B.; Talmon, Y.; Schmidt, J.; Cohen, Y.; Frimer, A. A. Active Oxygen Chemistry within the Liposomal Bilayer. Part III: Locating Vitamin E, Ubiquinol and Ubiquinone and their Derivatives in the Lipid Bilayer. *Chem. Phys. Lipids* **2004**, *131*, 107−121.
(36) Quinn, P. J. Is the Distribution of α-tocopherol in Membranes Consistent with its Putative Functions? *Biochemistry* **2004**, *69*, 58−66.
(37) Ricciarelli, R.; Zingg, J.-M.; Azzi, A. The 80th Anniversary of Vitamin E: Beyond its Antioxidant Properties. *Biol. Chem.* **2002**, *383*, 457−465.
(38) Rifici, S.; D'Angelo, G.; Crupi, C.; Branca, C.; Nibali, V. C.; Corsaro, C.; Wanderlingh, U. Influence of Alcohols on the Lateral Diffusion in Phospholipid Membranes. *J. Phys. Chem. B* **2016**, *120*, 1285−1290.
(39) Kranenburg, M.; Vlaar, M.; Smit, B. Simulating Induced Interdigitation in Membranes. *Biophys. J* **2004**, *87*, 1596−1605.
(40) Rowe, E. S.; Campion, J. M. Alcohol Induction of Interdigitation in Distearoylphosphatidylcholine: Fluorescence Studies of Alcohol Chain Length Requirements. *Biophys. J* **1994**, *67*, 1888−1895.
(41) Yin, H.; Lei, S.; Zhu, S.; Huang, J.; Ye, J. Micelle-to-Vesicle Transition Induced by Organic Additives in Catanionic Surfactant Systems. *Chem.—Eur. J.* **2006**, *12*, 2825−2835.
(42) Karayil, J.; Kumar, S.; Hassan, P. A.; Talmon, Y.; Sreejith, L. Microstructural transition of aqueous CTAB micelles in the presence of long chain alcohols. *RSC Adv.* **2015**, *5*, 12434−12441.
(43) Sreejith, L.; Parathakkat, S.; Nair, S. M.; Kumar, S.; Varma, G.; Hassan, P. A.; Talmon, Y. Octanol-Triggered Self-Assemblies of the CTAB/KBr System: A Microstructural Study. *J. Phys. Chem. B* **2011**, *115*, 464−470.
(44) Jia, X.; Chen, J.; Wang, B.; Liu, W.; Hao, J. Molecular dynamics simulation of shape and structure evolution of preassembled cylindrical cetyltrimethylammonium bromide micelles induced by octanol. *Colloids Surf., A* **2014**, *457*, 152−159.
(45) Ho, C.; Stubbs, C. D. Effect of n-Alkanols on Lipid Bilayer Hydration. *Biochemistry* **1997**, *36*, 10630−10637.
(46) Duhem, N.; Danhier, F.; Pourcelle, V.; Schumers, J.-M.; Bertrand, O.; LeDuff, C. S.; Hoeppener, S.; Schubert, U. S.; Gohy, J.-F.; Marchand-Brynaert, J.; Préat, V. Self-Assembling Doxorubicin−Tocopherol Succinate Prodrug as a New Drug Delivery System: Synthesis, Characterization, andin Vitroandin VivoAnticancer Activity. *Bioconjugate Chem.* **2014**, *25*, 72−81.
(47) Anderson, R. A.; Polack, A. E. The stability of sucrose monolaurate: rate of formation of lauric acid. *J. Pharm. Pharmacol.* **1968**, *20*, 249−254.
(48) Ferrer-Tasies, L.; Moreno-Calvo, E.; Cano-Sarabia, M.; Aguilella-Arzo, M.; Angelova, A.; Lesieur, S.; Ricart, S.; Faraudo, J.; Ventosa, N.; Veciana, J. Quatsomes: Vesicles Formed by Self-Assembly of Sterols and Quaternary Ammonium Surfactants. *Langmuir* **2013**, *29*, 6519−6528.
(49) Roy, A.; Dutta, R.; Banerjee, P.; Kundu, S.; Sarkar, N. 5-Methyl Salicylic Acid-Induced Thermo Responsive Reversible Transition in Surface Active Ionic Liquid Assemblies: A Spectroscopic Approach. *Langmuir* **2016**, *32*, 7127−7137.
(50) Mandal, S.; Kuchlyan, J.; Ghosh, S.; Banerjee, C.; Kundu, N.; Banik, D.; Sarkar, N. Vesicles Formed in Aqueous Mixtures of Cholesterol and Imidazolium Surface Active Ionic Liquid: A Comparison with Common Cationic Surfactant by Water Dynamics. *J. Phys. Chem. B* **2014**, *118*, 5913−5923.
(51) Villeneuve, M.; Ootsu, R.; Ishiwata, M.; Nakahara, H. Research on the Vesicle−Micelle Transition by ^{1}H NMR Relaxation Measurement. *J. Phys. Chem. B* **2006**, *110*, 17830−17839.
(52) Ghosh, S.; Ghatak, C.; Banerjee, C.; Mandal, S.; Kuchlyan, J.; Sarkar, N. Spontaneous Transition of Micelle−Vesicle−Micelle in a mixture of Cationic Surfactant and Anionic Surfactant-like Ionic Liquid: A Pure Nonlipid Small Unilamellar Vesicular Template Used for Solvent and Rotational Relaxation Study. *Langmuir* **2013**, *29*, 10066−10076.
(53) Ingólfsson, H. I.; Andersen, O. S. Alcohol's Effects on Lipid Bilayer Properties. *Biophys. J.* **2011**, *101*, 847−855.
(54) Nazari, M.; Kurdi, M.; Heerklotz, H. Classifying Surfactants with Respect to Their Effect on Lipid Membrane Order. *Biophys. J.* **2012**, *102*, 498−506.
(55) van Rheenen, J.; Achame, E. M.; Janssen, H.; Calafat, J.; Jalink, K. PIP2 signaling in lipid domains: a critical re-evaluation. *EMBO J.* **2005**, *24*, 1664−1673.
(56) Oseni, A. O.; Butler, P. E.; Seifalian, A. M. Optimization of chondrocyte isolation and characterization for large-scale cartilage tissue engineering. *J. Surg. Res.* **2013**, *181*, 41−48.
(57) Sarkar, S. D.; Farrugia, B. L.; Dargaville, T. R.; Dhara, S. Physico-chemical/biological properties of tripolyphosphate cross-linked chitosan based nanofibers. *Mater. Sci. Eng., C* **2013**, *33*, 1446−1454.

DOI: 10.1021/acsomega.7b00744
ACS Omega 2017, 2, 7637−7646